PROCEEDINGS OF SCIENCE

# The form factors for the rare decay $B \to K\ell^+\ell^-$ from three-flavor lattice QCD

**Rajendra D. Jain** *
*Deptartment of Physics, University of Illinois, Urbana, Illinois USA*
*E-mail:* rdjain1@uiuc.edu

**Fermilab Lattice QCD Collaboration**

We present preliminary results of a first lattice calculation of the form factors for the rare decay $B \to K\ell^+\ell^-$. Hadronic matrix elements are calculated on MILC lattices with 2+1 flavors of sea quarks. We use the Asqtad action for light quarks and the Fermilab action for the *b* quark.

*XXIVth International Symposium on Lattice Field Theory*
*July 23-28, 2006*
*Tucson, Arizona, USA*

*Speaker.

 

PoS(LAT2006)085

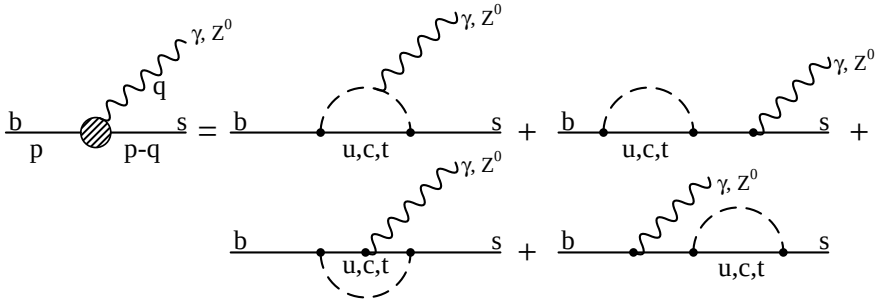


**Figure 1:** Penguin diagrams contributing to $B \to K\ell^+\ell^-$

## 1. Introduction

The rare decay $B \to K\ell^+\ell^-$ is a flavor-changing neutral current process. Like other such processes, it can provide important constraints on physics beyond the Standard Model. In particular, it may yield constraints which are complimentary to those provided by $B \to X_s\gamma$, since it probes additional operators. Its total branching fraction has recently been measured, and Belle finds [1] that $\mathrm{B}(B \to K\ell^+\ell^-) = (0.55 \pm 0.08) \times 10^{-6}$, while BABAR finds [2] $\mathrm{B}(B \to K\ell^+\ell^-) = (0.34 \pm 0.08) \times 10^{-6}$. A determination of the differential decay rate for this process, which is essential for a precision comparison with SM theory, may soon be within the reach of the current generation of $B$ factories.

## 2. Continuum Theory

The leading-order contributions to the $B \to K\ell^+\ell^-$ rate come from the electroweak penguin diagrams shown in Figure 1. Carrying out an operator product expansion yields effective hamiltonians for $b \to \gamma s$ and $b \to Zs$ transitions given by [3]

$$H^{eff.}_{bZ^\mu s} = -i \sum_{i=u,c,t} V^*_{ib}V_{is} \frac{G_F}{\sqrt{2}} \frac{e}{2\pi^2} M_Z^2 \tan(\Theta_W) F_Z(x_i) [\bar{b}_L \gamma^\mu s_L] \tag{2.1}$$

and

$$H^{eff.}_{b\gamma^\mu s} = -i \sum_{i=u,c,t} V^*_{ib}V_{is} \frac{G_F}{\sqrt{2}} \frac{e}{8\pi^2} \{F_\gamma(x_i)[\bar{b}_L(q^2\gamma^\mu - q_\mu \not{q})s_R] + F'_\gamma(x_i)[\bar{b}_L(im_b\sigma^{\mu\nu}q_\nu)]s_R\} \tag{2.2}$$

where the $F(x_i)$'s are known functions of $x_i \equiv m_i^2/m_W^2$. Hence, the hadronic matrix elements needed for $B \to K\ell^+\ell^-$ are $\langle B|\bar{b}\gamma^\mu s|K\rangle$ and $\langle B|\bar{b}\sigma^{\mu\nu}q_\nu s|K\rangle$. These have the standard parameterizations

$$\langle B(p)|\bar{b}\gamma^\mu s|K(k)\rangle = f_+(p^\mu + k^\mu - \frac{m_B^2 - m_K^2}{q^2}q^\mu) + f_0 \frac{m_B^2 - m_K^2}{q^2} q^\mu \tag{2.3}$$

and

$$\langle B(p)|\bar{b}\sigma^{\mu\nu}q_\nu s|K(k)\rangle = i\frac{f_T}{m_B+m_K}\left\{(p+k)^\mu q^2 - q^\mu(m_B^2-m_K^2)\right\}\ , \tag{2.4}$$

where $f_+$, $f_0$, and $f_T$ are $q^2$-dependent form factors for which we seek a lattice prediction.

## 3. Lattices and Actions

The results we present employ an ensemble of 460 MILC configurations with 2+1 flavors of dynamical sea quarks. The light valence and sea quarks are simulated using the Asqtad action, while for the $b$ we use the Fermilab action. The Fermilab action is $O(a)$ improved, while the Asqtad and gauge field actions have errors starting at $O(\alpha_s a^2, a^4)$. Within this formalism, the tree-level $O(\Lambda_{qcd}/m_b)$ errors which appear in two-quark heavy-light current operators can be removed through a simple spinor rotation of the heavy-quark field [4]. Results presented here are for $a = 0.12$ fm and $\kappa_b = 0.086$, with $am_\ell = 0.020$ and $am_s = 0.050$ for the sea quarks. For the valence quarks, $am_l = 0.020$, while $am_s = 0.0415$.

## 4. Extracting Matrix Elements

We calculate the matrix elements introduced in Section 2 in the $B$ meson rest frame at various kaon momenta, $\mathbf{p}$. In the calculation of three-point functions, the $K$ was created at $T_{source} = 0$ while the $B$ was destroyed at $T_{sink} = 16$. The relevant correlators can be written as

$$\begin{aligned} C_{2H}(\mathbf{p};\, t) &\equiv \sum_{\mathbf{x}} e^{-i\mathbf{p}\cdot\mathbf{x}}\left\langle H^\dagger(0)H(\mathbf{x},t)\right\rangle \\ &= \sum_k Z^2_{H_k}(\mathbf{p})e^{-E_{H_k}(\mathbf{p})t} + \sum_l (-1)^t Z^2_{H'_l}(\mathbf{p})e^{-E_{H'_l}(\mathbf{p})t} \end{aligned} \tag{4.1}$$

where $H$ is one of the interpolating fields $B \equiv \bar{b}\gamma^5 d$ or $K \equiv \bar{s}\gamma^5 d$ and

$$\begin{aligned} C_{3\Gamma}(\mathbf{p};\, t, T_{sink}) &\equiv \sum_{\mathbf{x},\mathbf{y}} e^{-i\mathbf{p}\cdot\mathbf{x}}\left\langle K^\dagger(0)\,\bar{s}(\mathbf{x},t)\Gamma b(\mathbf{x},t)B(\mathbf{y},T_{sink})\right\rangle \\ = \sum_j \left[\sum_k A^{(jk)}_\Gamma(\mathbf{p})e^{-E_{K_j}t}e^{-E_{B_k}(T_{sink}-t)} + \sum_l (-1)^t B^{(jl)}_\Gamma(\mathbf{p})e^{-E_{K_j}t}e^{-E_{B_l}(T_{sink}-t)}\right] \end{aligned} \tag{4.2}$$

where $\Gamma$ is one of either $\gamma^\mu$ or $\sigma^{\mu\nu}$ and the summation indices $j,k$, and $l$ run over the tower of meson states which contribute to each correlation function. The appearance of oscillating terms in the $C_2$ and $C_3$'s is due to the use of naive valence quarks [5]. Note that in our expansion of the three-point functions, we have not yet included contributions coming from oscillating kaon states as contributions from these states are found to be small in the $K$ two-point functions. The ground-state matrix elements of interest are given in terms of the above parameters according to

$$\langle K(\mathbf{p})|\,\bar{s}\Gamma b\,|B(\mathbf{0})\rangle = A^{00}_\Gamma/(Z_{B_0}Z_{K_0})\ . \tag{4.3}$$

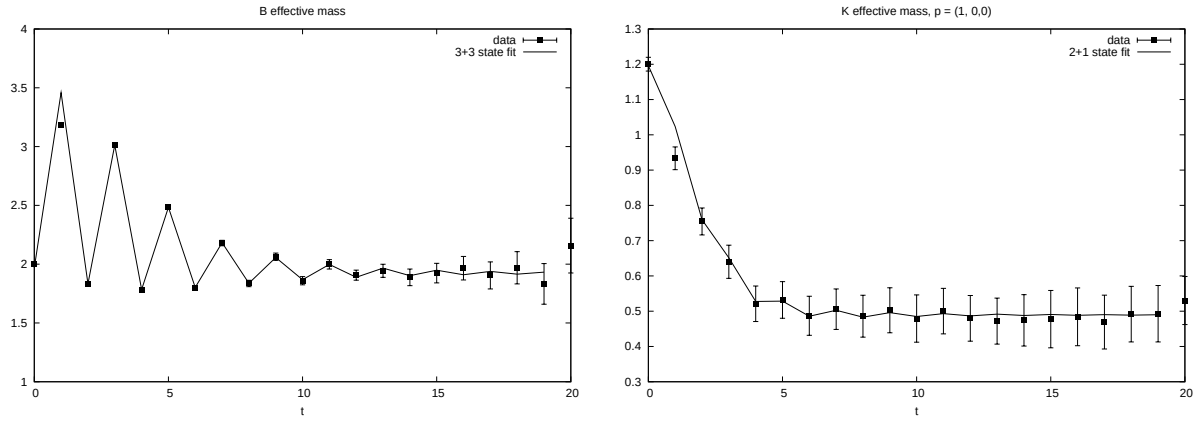


**Figure 2:** Fits to two-point correlators

## 5. Fitting procedure

The parameters $Z$, $A$, and $B$ described above, as well as the energies of the various states are extracted from lattice data through a simultaneous fit to two- and three- point correlators. We use a constained curve fitting method with Bayesian priors.

We first fit the two-point data alone in order to extract energy and overlap parameters for the various meson states. Next, for each $\Gamma$ we performed simultaneous fits to the two-and three-point functions checking where possible that fit parameters remained consistent with the individual two-point fits. Typically, the energy and overlap parameters of the meson states were unchanged to within less than one sigma.

Examples of our fit results are shown in Figures 2 and 3. On the left in Figure 2 is a 3+3 state fit (3 "regular" states and 3 oscillators) to the $B$ meson propagtor at zero momentum, while on the right is a 2+1 state fit to the $K$ propagator at lattice momentum $\mathbf{p} = (1,0,0)$. The fit range in our two-point fits was chosen to be $2 < t < 15$ giving $\chi^2$'s typically of about 0.5.

In Figure 3 we see fits to the three-point functions with the leading exponential time-dependence factored out. On the left is a fit to the $C_{3V^4}(\mathbf{p}_K = 0,0,0)$ correlator including contributions from 2 regular $B$ states, 2 $B$ oscillators, and a single regular kaon state (a "2+2+1" state fit). On the right is a 2+2+2 state fit to the $C_{3\sigma^{14}}(\mathbf{p}_K = 1,0,0)$ correlator. The typical fit range was $5 < t < 14$. Work on determining the optimal fitting strategy for this calculation is still in progress. With better statistics and the inclusion of more states in our fits, we plan to study in more detail the fit systematics with the hope of increasing the range in $t$ over which we can fit.

## 6. From Matrix Elements to Form Factors

The matrix elements calculated from lattice correlators are related to their continuum counterparts through current renormalization. Following [6], we factor this renormalization into two parts:

$$J_\Gamma^{cont.} \equiv (\bar{s}\Gamma b)^{cont.} = \sqrt{Z_V^{hh} Z_V^{ll}}\rho_\Gamma J_\Gamma^{lat.} \tag{6.1}$$

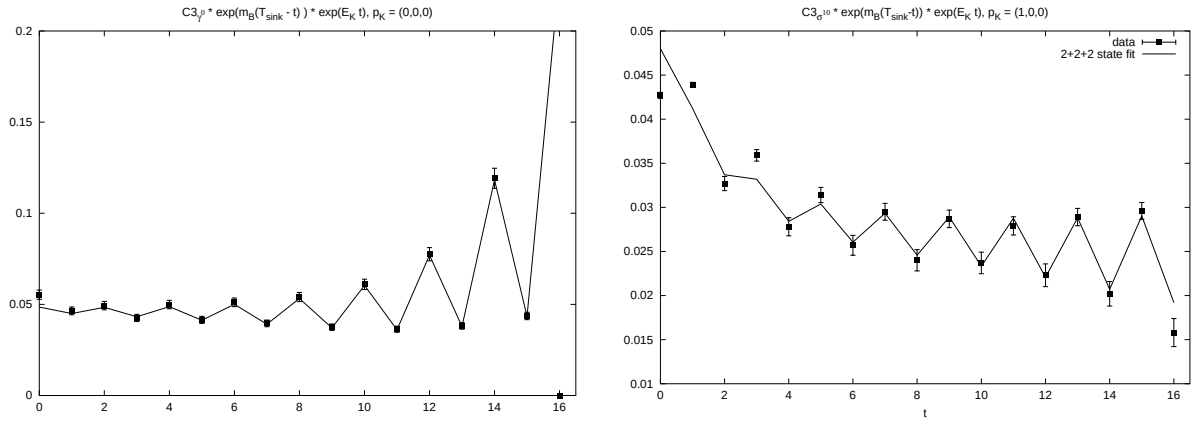


**Figure 3:** Fits to three-point correlators

where $Z_V^{hh}$ and $Z_V^{ll}$ are non-perturbative renormalization factors which are being calculated within our collaboration. The vector current $\rho$'s have been calculated [7] and are very close to unity, while the $\rho_\sigma$'s remain to be computed. In this work, we use the values $Z_V^{hh} = 2.995$ and $Z_V^{ll} = 0.884$ [8], while for simplicity we take each $\rho = 1$.

The form factors introduced in Section 2 can then be related to these matrix elements according to

$$f_0(q^2) = \frac{1}{m_B^2 - m_K^2}\left[(m_B - E)\langle K|V^4|B\rangle + \sum_{i=1}^{3}(E^2 - m_K^2)\frac{\langle K|V^i|B\rangle}{p_i}\right], \tag{6.2}$$

$$f_+(q^2) = \frac{1}{2m_B}\left[\langle K|V^4|B\rangle + (m_B - E)\frac{\langle K|V^i|B\rangle}{p_i}\right] \tag{6.3}$$

and

$$f_T(q^2) = -i\frac{m_B + m_K}{2m_B q^2}\left[\langle K|\sum_{j=i}^{3}\sigma^{4j}p_j|B\rangle + (m_B - E)\sum_{j=1}^{3}\frac{\langle K|\sum_{\mu\neq j}\sigma^{j\mu}p_\mu|B\rangle}{p_j}\right]. \tag{6.4}$$

For the kaon energy, $E$, we use the fitted rest mass, $m_K$, and the continuum dispersion relationship $E^2 = m_K^2 + p^2$, while for the $B$-meson mass we use the measured value from the PDG.

## 7. Results

The results obtained for the form factors $f_0$ and $f_+$ introduced in section 2 are shown in Figure 4. The analysis needed to extract $f_T$ is still a work in progress. It should be emphasized that these results are preliminary as we have not yet finalized our fitting procedure or quantified the systematic uncertainties therein. Errorbars represent statistical errors alone, extracted through a jacknife analysis of the lattice data.

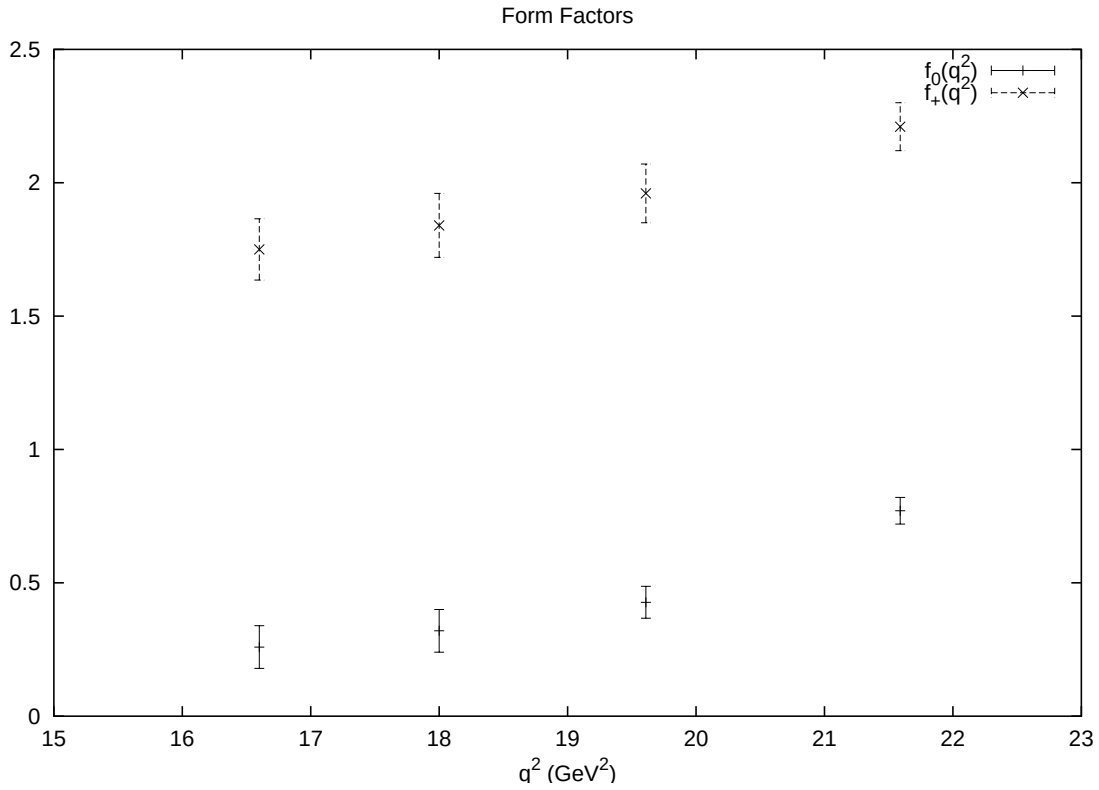


**Figure 4:** Form factors contributing to $B \to K\ell^+\ell^-$

## 8. Conclusion and Outlook

We have presented preliminary results for two of the form factors for $B \to K\ell^+\ell^-$ from lattice QCD and are in the process of computing the third. The first step in improving our analysis will be to study the systematic errors introduced by fitting. We plan to study in detail the robustness of our procedure, as well as to explore alternate methods such as fitting to a ratio of correlators as has been done elsewhere in our collaboration. It is hoped that by using multiple time-sources, as well as combining smeared and unsmeared data, we can reduce statistical errors, allowing us to better constrain excited states and to improve the quality of our fits. Additionally, we plan to compute the perturbative corrections to the tensor current operators at one-loop. Finally, this analysis will also need to be repeated on other MILC ensembles so that we can study the lattices spacing and light-quark mass dependence of our results.

## 9. Acknowledgements

The numerical simulations for this work were carried out on the Fermilab lattice QCD clusters, which are a computing resource of the USQCD collaboration and are funded by the DOE. I am grateful to the Fermilab Computing Division for operating and maintaining the clusters, as well as

to Ruth Van de Water, James Simone, and Aida El-Khadra for their helpful discussions. This work was supported in part by the DOE under grant no. DE-FG02-91ER40677.

## References

[1] K. Abe *et. al.* [Belle Collaboration], [arXiv:hep-ex/0410006]

[2] B. Aubert *et. al.* [BaBar Collaboration], [arXiv:hep-ex/0507005].

[3] T. Inami and C.S. Lim, Prog. Theor. Phys. **65**, 297 (1981).

[4] A. X. El-Khadra, A. S. Kronfeld and P. B. Mackenzie, Phys. Rev. D **55** (1997) 3933 [arXiv:hep-lat/9604004].

[5] M. Wingate, J. Shigemitsu, C. T. H. Davies, G. P. Lepage and H. D. Trottier, Phys. Rev. D **67** (2003) 054505 [arXiv:hep-lat/0211014].

[6] J. Harada, S. Hashimoto, K. I. Ishikawa, A. S. Kronfeld, T. Onogi and N. Yamada, "Application of heavy-quark effective theory to lattice QCD. II: Radiative Phys. Rev. D **65** (2002) 094513 [Erratum-ibid. D **71** (2005) 019903] [arXiv:hep-lat/0112044].

[7] M. Nobes, work in progress

[8] J. Simone, private comm. (2006)